



## ACODEPT

### Advanced Coil Design for Electromagnetic Pulse Technology

#### Project partners



University of Gent – Department Electrical Energy, Systems and Automation

A. Van den Bossche, D. Bozalakov

[www.ugent.be/ea/eesa/en](http://www.ugent.be/ea/eesa/en)



Chemnitz University of Technology, Chair of Microsystems and Precision Engineering

V. Kolchuzhin, J. Mehner

[www.tu-chemnitz.de](http://www.tu-chemnitz.de)



Fraunhofer Institute for Machine Tools and Forming Technology

V. Psyk, C. Scheffler, W.-G. Drossel

[www.iwu.fraunhofer.de](http://www.iwu.fraunhofer.de)



Belgian Welding Institute

K. Faes

[www.BIL-IBS.be](http://www.BIL-IBS.be)



European Association of Sheet Metal Working (EFB)

Dr.-Ing. Norbert Wellmann

[www.efb.de](http://www.efb.de)

#### Abstract

To make the advantages of electromagnetic forming applicable for industrial manufacturing, a three step design strategy for tool coils is suggested. At first, simplified decoupled electromagnetic and structural mechanical simulations are used for creating a preliminary design via a systematic iterative optimisation process. The selected design is verified in more accurate coupled simulations. A prototypic realisation serves for further optimization, if necessary. The applicability of the approach is proved on the basis of an inductor system for cutting and forming of sheets and for magnetic pulse welding of tubes.

## Project summary

### Electromagnetic pulse technology

Electromagnetic forming (EMF) is a relative new and attractive technology, which can be used for joining, welding, forming and cutting of metals. The technology is based on the utilisation of electromagnetic forces and offers attractive possibilities for:

- obtaining a larger deformation of some materials, in comparison with conventional forming, while avoiding the disadvantages of the conventional processes,
- fast and cost-effective joining of non-weldable materials, like heterogeneous joints;
- creating complex or new workpieces and products, impossible by conventional technologies,
- improving the working conditions of the welders or operator, since EMF is environmentally clean (no heat, fumes, shielding gases, radiation, etc.).

The critical part of the technology is the coil, which is always application-specific designed. When inappropriately designed or constructed, these parts fail very quickly, or low process efficiency is obtained. Durable, robust and efficient coil systems are however essential for a successful implementation of EMF in industry.

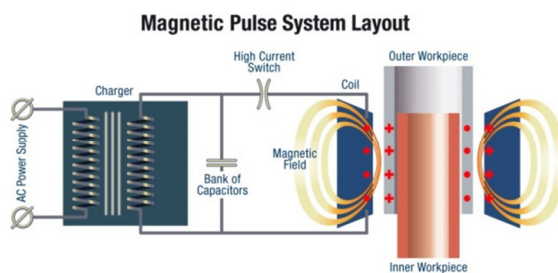


**Figure 1:** Principle of the EMF for tubular products

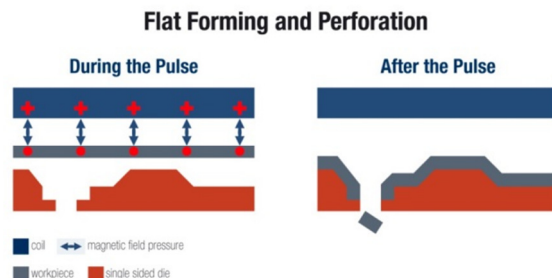


**Figure 2:** Principle of the EMF for sheet metal forming and cutting

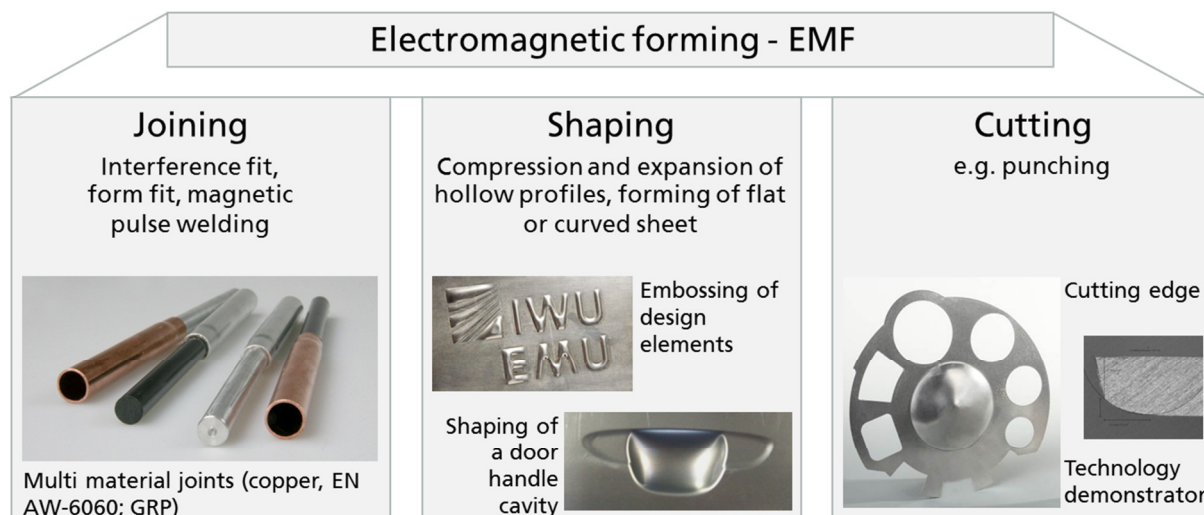


**Figure 3:** Fields of applications of EMF

### Project objectives

Currently, the knowledge concerning coil design is dispersed among the pulse machine manufactures, often confidential and thus not available for end users. One of the aims of the project is to develop all necessary knowledge to provide SMEs and other companies the flexibility to design



and manufacture coils for specific applications. This will lead to an increased use and applicability of EMF in the metal processing industry.

The technical targets aimed at in this project are:

- Development of finite-element models, which will increase the knowledge about the process and which will serve as a tool in the coil design process.
- Methodology for designing coils for forming and cutting of sheets and forming and welding of tubular workpieces.
- Guidelines for manufacturing, material selection, insulation strategy and other construction-related aspects.
- Providing the companies with all essential information to make a considered decision about the successful integration of the EMF and related technologies in their production.

Although most advantages have been known for a long time, still no large industrial breakthrough of the process is achieved. One of the reasons is the restrictions considering design and manufacturing of durable inductors. Knowledge about this is mainly confidential property of equipment manufactures. Systematic means directly applicable for the process and tool design for specific application cases are still missing. Therefore, the aim of this project is contributing to closing this gap.

The experimental research using pulsed-power equipment was performed by Fraunhofer IWU and the Belgian Welding Institute. EELAB of the Ghent University used its expertise in the field of calculation of magnetic forces, current density, etc. in order to calculate the desired shape of the coil systems. Finite-element modelling of the process was performed by the University of Chemnitz.

## **Design strategy for inductor systems for electromagnetic forming technologies**

The fact that mechanical, electromagnetic, and thermal fields interact with each other and in principle mutual influences must be considered complicates process and tool design for EMF. Considering interactions with the thermal field is mandatory only if local temperature peaks occur due to strain localisation or significant resistive heating. The ideal solution for designing inductor systems is modelling the process in a 3D-coupled simulation, which allows estimating functionality of the inductor as well as quantifying acting loads and drawing conclusions regarding durability. However, this procedure is hindered because currently no fully developed simulation software is available for such a complex simulation. The current restrictions are :

- calculation costs for coupled simulations are high, so that comprehensive parameter studies, which are necessary for the ideal design process, cannot be realised reasonably.
- usually the simulation codes are limited to forming applications. Coupled simulation tools for modelling joining/welding or cutting operations are even less developed.
- material data for accurate modelling as flow-curves at high strain rates and high strains, appropriate parameters for damage modelling, etc. is hardly available.

To overcome the first two of these restrictions, the following innovative design strategy consisting of three subsequent steps was suggested by Fraunhofer :

1. In the first step, a simplified approach is used for developing a preliminary design of the inductor system, considering mechanical and electromagnetic aspects of the process separately. Here, simplified analytical correlations as well as uncoupled simulation tools can be applied. This allows performing comprehensive parameter studies and pre-selecting promising designs.



2. In the second step, these selected designs are further evaluated by more accurate coupled simulations.
3. Finally, experimental verification of the simulation using a prototype inductor allows further optimisation of the tool. The strength of this design strategy is that the optimising effort can be adapted to the operative conditions and the specific manufacturing task. If time and costs are extremely limited, an applicable inductor concept is available already after the first design step. For complex tasks and high-volume production, higher optimisation effort should be made to meet the high demands on the tool.

## Preliminary design of the inductor system

### Application-oriented requirements and deduction of a suitable pressure pulse

As a first step in the design process, the demands to be made on the inductor system have to be identified as precisely as possible. For this purpose, at first application-related requirements are defined. Depending on the application, these requirements vary significantly. In case of forming, the major issue is probably good form-filling. In case of cutting, the size and shape of the cut-out are decisive. For welding the required impacting parameters are relevant. In the next step, these application-oriented requirements have to be abstracted to that extent that a suitable pressure pulse, characterised by its rise-time, maximum, and local distribution is identified as target value. For this purpose, numerical parameter studies can be performed.

### Draft geometry of an inductor system providing the desired pressure pulse

Finding a suitable inductor system that together with the pulsed power generator provides the required pressure pulse is probably the most challenging aspect of the design process. To allow an efficient approach, a systematic iterative optimisation procedure illustrated in Figure 4 was developed.

For evaluating and iteratively adapting the inductor system, the magnetic field must be calculated. In most cases, a numerical electromagnetic simulation will be required for this purpose and the inductor current, which is a priori not known, might be necessary input data. In this case, a sinusoidal course with estimated values for amplitude and frequency can be assumed. Reasonable values for the frequency of discharging current usually are in the magnitude of 5-15 kHz.

Since a more substantial approximation of the current course is integrated as a part of the design process, even starting with values far from the target will lead to the desired result, although additional iteration loops might be necessary.

The corresponding magnetic pressure  $p$  is calculated based on the magnetic permeability  $\mu$ , the magnetic field in the gap between inductor system and workpiece  $H_{gap}$  and the magnetic field on the workpiece surface facing away from the inductor system  $H_{pen}$  via the equation below.

$$p = \frac{1}{2} \cdot \mu \cdot (H_{gap}^2 - H_{pen}^2)$$

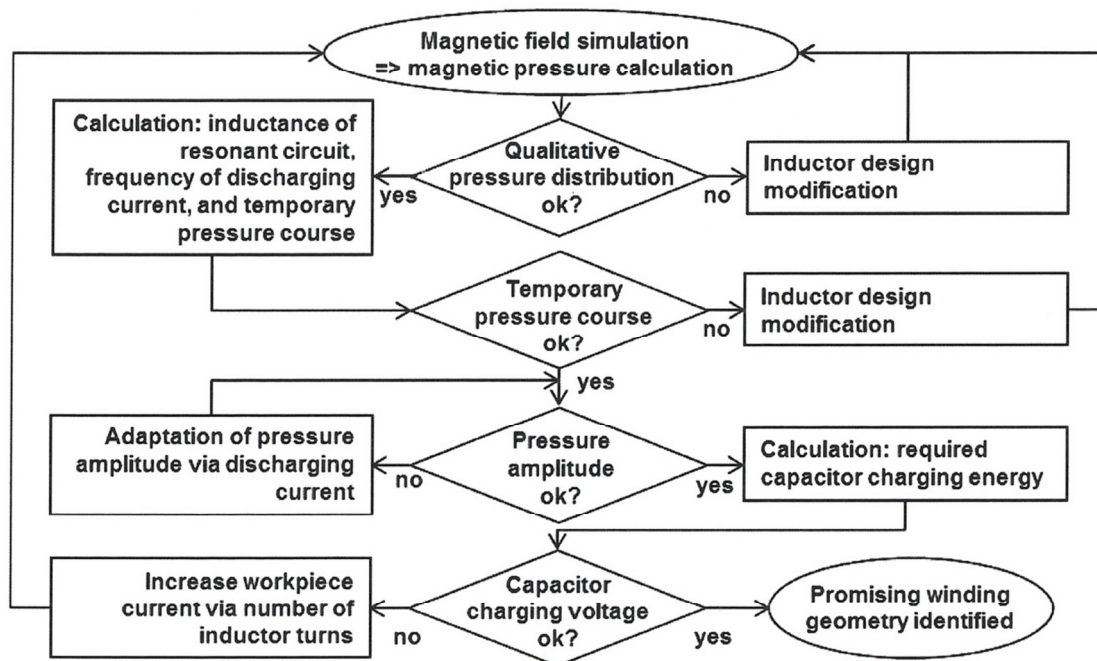


**Figure 4:** Flow-chart for pressure oriented evaluation and adaptation of the inductor system

The calculated pressure distribution is qualitatively compared to the target pressure pulse identified above. If modifications are required, they can be realised via geometric adaptations of the inductor system geometry.

For direct acting coils (i.e. without a fieldshaper), local pressure reduction can be achieved by reducing the density of turns via increasing either the width of individual turns or the gap between neighbouring turns. However, large gaps lead to drastic local pressure reduction in-between individual turns. Pressure reduction via an increase of the gap between inductor and workpiece in principle is possible, but leads to lower process efficiency, so that generally this gap should be as small as the necessary insulation allows.

For setups with fieldshapers, a qualitative adaptation of the pressure profile can be achieved by slight changes of the geometry in the concentrating area. Again, increasing the gap results in lower magnetic pressure and vice versa. However, also here increasing this gap decreases process efficiency.

If the qualitative pressure distribution approximates the target pressure pulse well enough, a more substantial estimation of the inductor current is required. The challenge is that the frequency of the discharging current and the inductance of the resonant circuit, consisting of the pulsed power generator, the inductor system and the workpiece, mutually influence each other and neither of them is known at this point.

For approximating both at the same time, an iterative calculation approach can be used. For this purpose, the calculated magnetic field distribution is interpreted regarding the common inductance of inductor system and workpiece  $L_{\text{consumer}}$ . Taking into account the inner inductance  $L_i$  and the capacitance of the pulsed power generator  $C$ , an updated value for the frequency of the discharging current  $f$  can be determined by the following equation.

$$f = \frac{1}{2\pi\sqrt{(L_{\text{consumer}} - L_i) \cdot C}}$$

Applying it in a new numerical calculation of the magnetic field, will lead to an iterative improvement of the determined consumer inductance. With increasing number of iterations, the alteration of the inductance and frequency will steadily decrease. A change of the frequency of less than 0,5 kHz from one iteration step to the next can be considered as a reasonable abort criterion.

On this basis, the course of the pressure pulse can be approximated. For small workpiece deformations, the inductance change due to the workpiece deformation is neglected at this stage of the design process. Thus, it can be assumed that the duration of the first pressure pulse corresponds to the duration of the first half-wave of the inductor current. In case of more significant workpiece deformations, it might be more appropriate to assume that the pressure pulse rises according to the square of the current rise and collapses abruptly when or even before the maximum value is reached. By this assumption, the overestimation of the magnetic pressure due to the decoupled view of the process is at least partly compensated. The deduced pressure course is then compared to the target pressure pulse. If a faster pressure pulse is required, suitable modification options include :

- reducing the number of turns of the inductor winding,
- choosing a pulsed power capacitor of lower capacitance and/or inner inductance, or
- if an inductor system including a field shaper is used, decreasing the winding diameter.

Slower pressure pulses can be realised by modifying the parameters in the other direction. For the modified inductor system, it has to be checked if the qualitative pressure distribution still fits with the target values.

Theoretically, a suitable inductor system is identified at this point, but it must be checked if it is fitting with practical technological boundary conditions, i.e. especially if the capacitor charging energy provided by the available pulsed power generator is sufficient to achieve the desired maximum pressure. Therefore, the current amplitude assumed in the simulations, which was irrelevant up to this point, has to be taken into consideration now. It must be successively increased or decreased until the resulting maximum magnetic pressure value corresponds to the target value.

The energy transferred to the consumer conforms to the capacitor charging energy  $E_c$  multiplied by an efficiency factor  $\eta$ , which depends on the equipment and on parameters as positioning of inductor and workpiece and can be estimated only roughly. Accordingly, the necessary capacitor charging energy and voltage  $U_c$ , respectively, leading to a defined maximum discharging current  $I_{max}$  can be approached via the equation below. If the required capacitor charging voltage cannot be realised with the available equipment, adding turns to the inductor can increase the current induced in the workpiece, so that higher pressure maxima are available for the same charging energies.

$$U_c = \sqrt{\frac{2 \cdot E_c}{C}} \quad \text{with} \quad E_c = \eta \cdot \frac{(L_{consumer} + L_i) \cdot I_{max}^2}{2}$$

### Improved tool design via coupled simulation

Altogether, the preliminary design procedure described above includes several simplifying assumptions and rough estimations, but since it is a tool for pre-selecting promising geometry variants only, such drastic simplifications are acceptable. Further evaluation of the selected designs by coupled simulations reduces the tentativeness of the design approach significantly.

Due to the decoupled consideration of electromagnetic and structural mechanical simulation within the preliminary design, especially all retroactivities of the workpiece deformation on the acting pressure pulse are disregarded. This leads to overestimation of the acting pressure, which



corresponds to the energy density of the magnetic field. Due to the increase of the gap between inductor system and workpiece, caused by the workpiece deformation, the magnetic field can expand to a larger volume, and thus the energy density and accordingly the acting pressure decrease. This is more relevant the more pronounced the deformation is and especially if it starts early during the pressure rise period.

Coupled simulation drastically reduces the resulting error, because the acting loads are calculated and applied in interaction to the deformations of the structural model, so that the retroactivity on the applied pressure is taken into account.

LS-DYNA R7 can be used for performing 3-dimensional stepwisely coupled simulations. This means that on the basis of the magnetic field simulation considering the initial setup, the acting forces are determined and applied to the mechanical model for a short period of time (i.e. a few microseconds). Here, the according workpiece deformation is analysed and serves as input data for an updated calculation of electromagnetic model. This data exchange is repeated until the acting forces faded or the workpiece deformation is completed.

In LS-DYNA R7, the structural mechanical system is calculated via Finite-Element-Methods (FEM), while in the electromagnetic model the Boundary-Element-Method (BEM) is used avoiding the meshing of the surrounding air and thus reducing the model size. Other coupled simulation approaches (e.g. Comsol or Ansys) calculate both systems via FEM, implicating additional problems regarding the remeshing of the surrounding air especially when different bodies contact each other and the air in-between them has to be eliminated. Since the inductor current is a priori not known, LS-DYNA R7 includes the possibility of using the electrical voltage and the characteristics of the pulsed power generator as alternative input data.

Coupled simulations are carried out for one or several selected design(s) according to the outcome of the preliminary design and interpreted with regard to the inductor current and the pressure pulse, which can be approached by integrating the forces acting on the nodes over the workpiece thickness and relating them to the according element size. Comparing the inductor current determined here with the one estimated in the preliminary design provides information about the error made in the first design step. A comparison of the pressure pulse calculated here to the target pressure serves for evaluating the specific design(s) of the inductor system.

## Exemplary design of inductor systems

### Manufacturing of a flat coil prototype for cutting and embossing

For the manufacturing of flat coil prototypes for performing the cutting and embossing (forming) of sheet metal components, it was decided to manufacture the windings as well as the insulation and housing components from individual components machined from conventional semi-finished parts.

To demonstrate possible applications of inductors of the Bitter coil type for flat forming and cutting applications, Fraunhofer developed two of these coils. In the ACODEPT project, the focus was put on cutting applications in the range of diameters 25 up to 120 mm. The developed "Coil50" is highly efficient for the diameter range of 35 up to 55 mm and the "Coil100" was designed for the range of 70 up to 100 mm. The principle coil design will probably be applicable also for slightly smaller and for larger diameters, but in those cases an adaptation of the coil measurement will be necessary.

As an alternative to helically wound flat coils which are frequently used without field shapers, it was decided to apply the cylindrical Bitter coil design because the investigated diameters are too small

for a successful application of helical flat coils. Based on pre-calculations, it was demonstrated that the use of a field shaper is expedient in order to make the cylindrical coil applicable for flat forming.

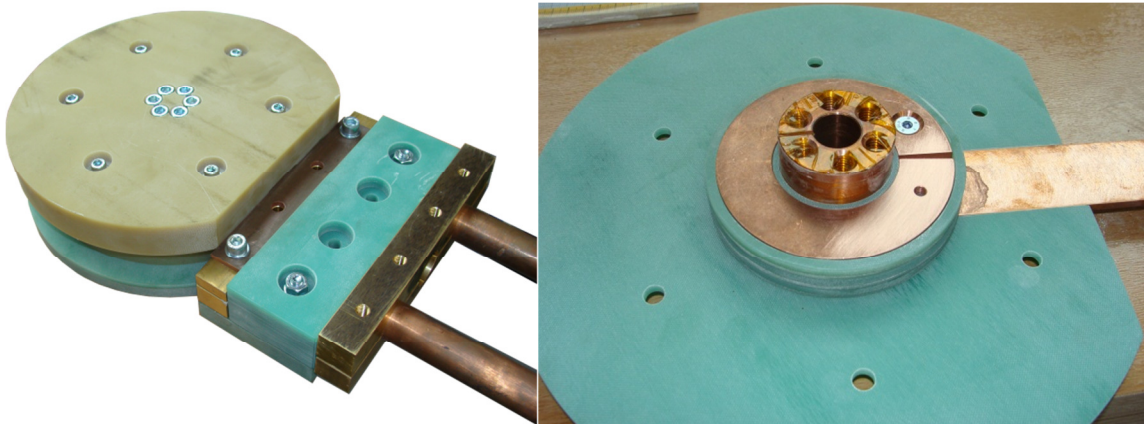


**Figure 5:** Left: Assembled cutting coil with feedings Right: During assembly

Because of the acting forces between the conductor plates (windings), the Bitter plate design needs a clamping force which fixes the conductor plates in axial and radial direction. In order to avoid bore holes for the clamping bolts which often go directly through the conductors and which often cause insulation problems and structure weakening, an alternative was developed where the force flux is closed by the field shaper itself. In this case, the windings are pressed together and the field shaper is set under tension which is mostly not a problem because of its stiff design. The screws between the windings are only for minor fixing of all the conductor plates and do not absorb any force.

Particular attention had to be paid to the insulation of critical points between the windings and the field shaper. The field shaper was insulated on its outside by Kapton foil but there still remain critical points.

In experiments by Fraunhofer, it turned out that the coils can be loaded with a voltage maximum of about 13 kV, which is at 28 kJ a current maximum of 262 kA for the “Coil50” or 210 kA for the “Coil100” without noteworthy problems. It was observed that the “Coil50” is more critical for a failure and flash over at lower voltages in particular at the field shaper and the windings, what is caused by higher loadings due to the smaller diameter.

The inductance of the coil and the system coil-workpiece is computed with the 3D model by LS-DYNA.

Theoretically, workpieces of higher electrical conductivity reduce the system inductance, so that in principle for the steel workpieces compared to the aluminium sheets a higher inductance can be expected. However, this effect is less pronounced, if a field shaper is included in the system and in the regarded cases this effect seems to be too weak to be recognized.

### Design of flat coils with a uniform pressure distribution

Considering the chosen application of embossing design elements, it can be supposed that a uniform pressure distribution is favourable in order to test different designs. Therefore, Fraunhofer IWU focused on flat forming with a so-called uniform pressure actuator.

Based on the patent DE 10 2005 013 539 A1 and US 2005/0217333 A1 of Glenn Daehn from Ohio State university, Fraunhofer developed an actuator featuring 7 rectangular turns made of milled copper-zirconium (CuCrZr) elements and insulated with Kapton film and Nomex paper. The core in the centre serves as insulation and absorbs compression forces. However, since the winding itself is relatively stiff, it was decided to use non-reinforced plastic, here.

The axial end covers serve for axially compressing the winding via the screws in the edge section. Here, they are made of glass fibre-reinforced plastic. In order to provide a more homogeneous loading of the covers and reduce the acting bending moment, additional steel plates can be added at the outer surface of the covers. In that case, probably a cheaper insulation material of lower strength would be sufficient for the cover manufacturing. Some pictures from the assembly of the first prototype of this coil type are shown in Figure 6.

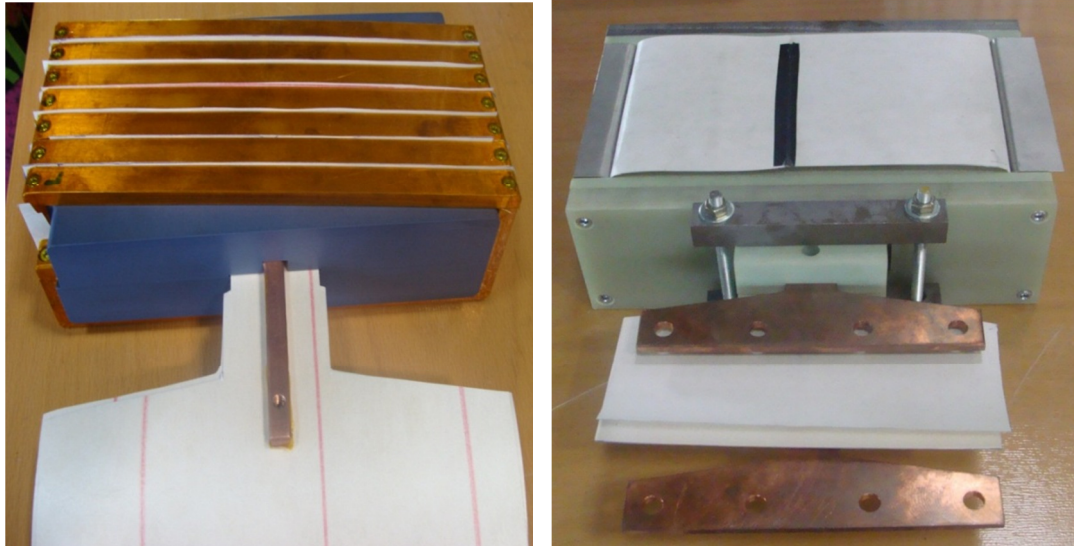


**Figure 6:** Assembly of the uniform pressure actuator. Left: Coil with core. Right: Complete coil with housing and conductive channel

The particularity of the uniform pressure actuator comes from the conductive channel which leads to a current flux going through the work piece and the conductive channel. This coil type features much better efficiency and more homogeneous pressure distribution comparing the achieved magnetic pressures at the same energy on the actuator without back iron, see Figure 7. The conductive channel has electrical contact to the work piece on both sides of the actuator, as depicted in Figure 7. It is made of steel in order to guarantee high strength. Inserted in this channel is an aluminium sheet, which serves as back path for the electrical current. Here the electrical conductivity is relevant in order to increase the efficiency of the inductor system, while the strength is not important here. The oxides and dirt at the contacting areas, where the current flows from the workpiece to the conductive channel and back have to be removed in order to reduce the contact resistance. High contact resistances lead to arcing and reduce the process efficiency. However, with increasing number of discharge processes the contacting surface of the conductive channel is deteriorated. Here it is advantageous that only the low-cost aluminium sheet needs to be exchanged, while the steel channel is not damaged at all.

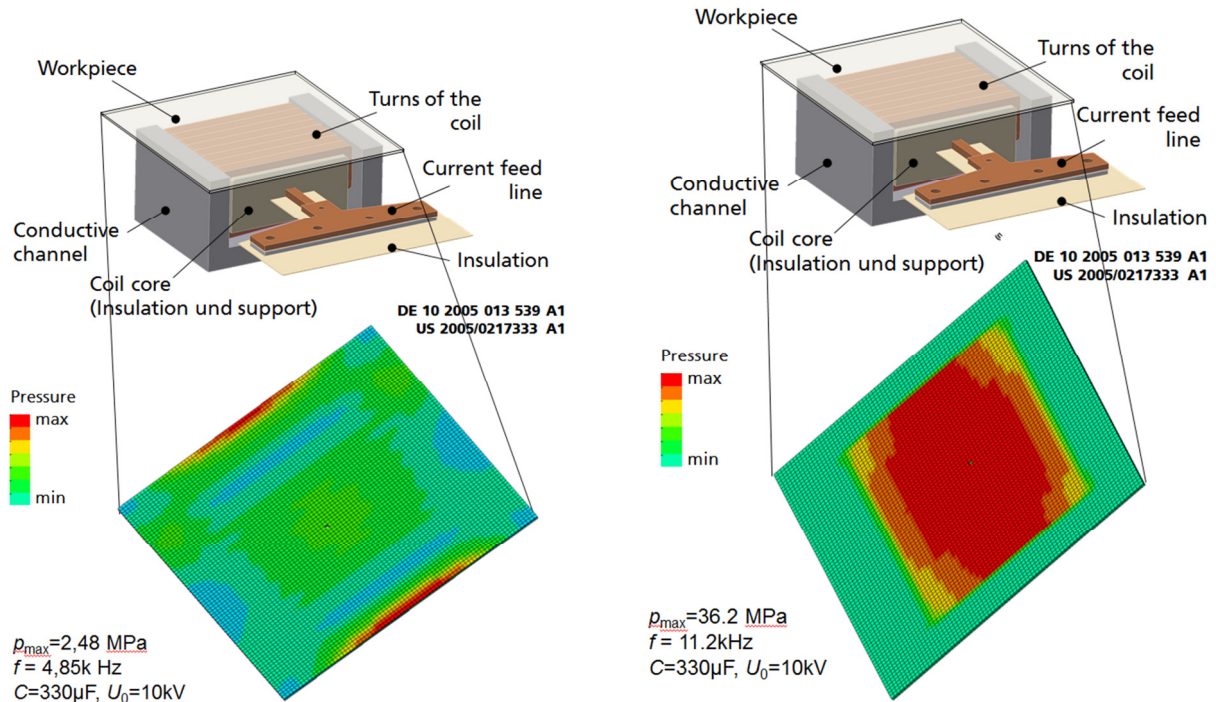


**Figure 7:** Characteristic of the uniform pressure actuator. Left: Pressure distribution (simulated) in case of electrical insulation between work piece and conductive channel. Right: Pressure distribution (simulated) in case of electrical contact of work piece and conductive channel

### Manufacturing of a cylindrical Bitter coil prototype

After analysis of the existing BWI Bitter coil (see Figure 8, right), a new Bitter coil has been designed and constructed. A Bitter coil is formed by stacking the alternating conductors and insulating discs, each foreseen with a radial cut. The neighbouring conductor parts form a spiral conducting path. The contact between the disks is realised due to their overlap. A simple assembly jig can be used to assemble the coil. A drawing is shown in Figure 9.

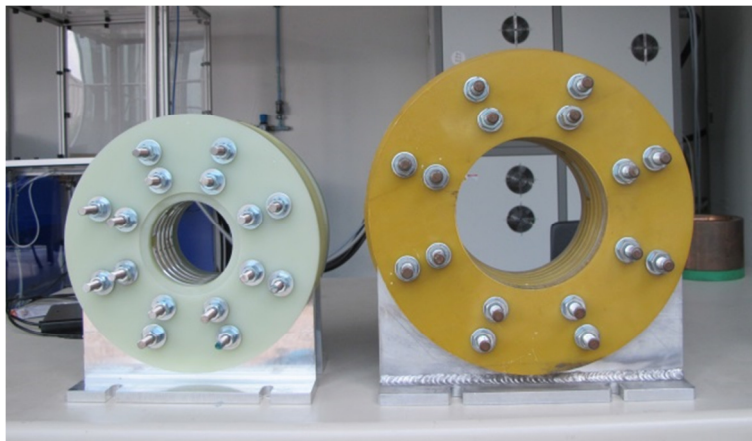


**Figure 8:** Left: New designed Bitter Coil - Right: Existing BWI Bitter coil

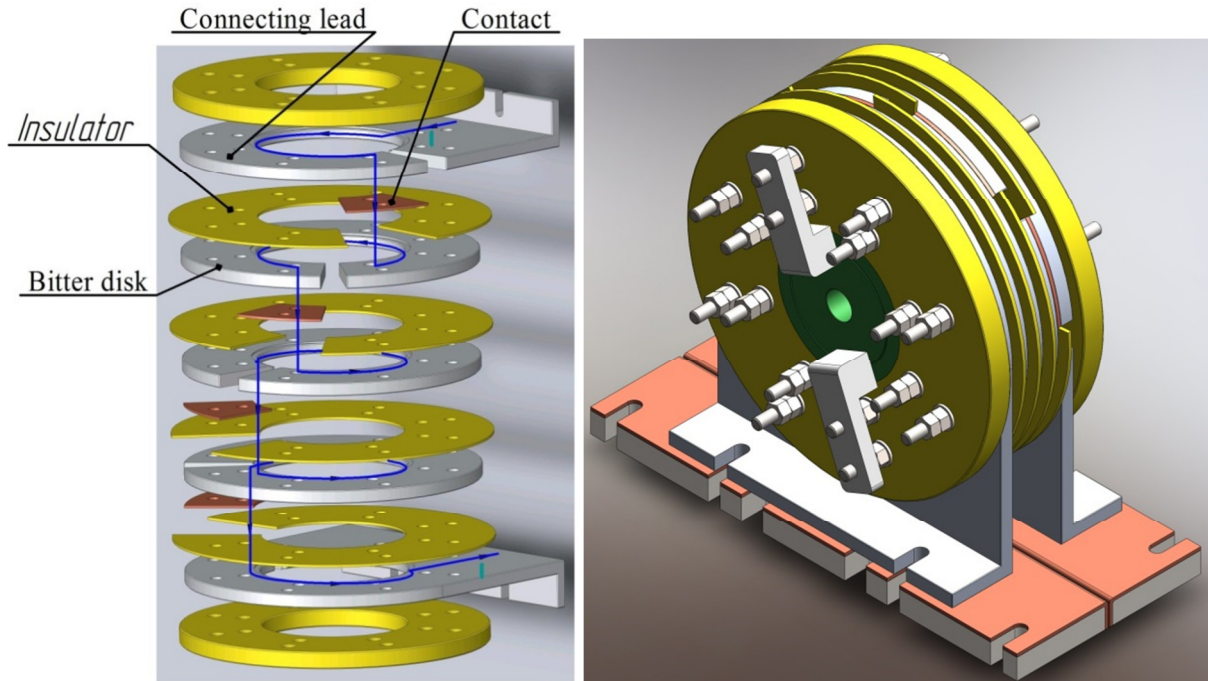


**Figure 9:** Principle drawing of the designed coil

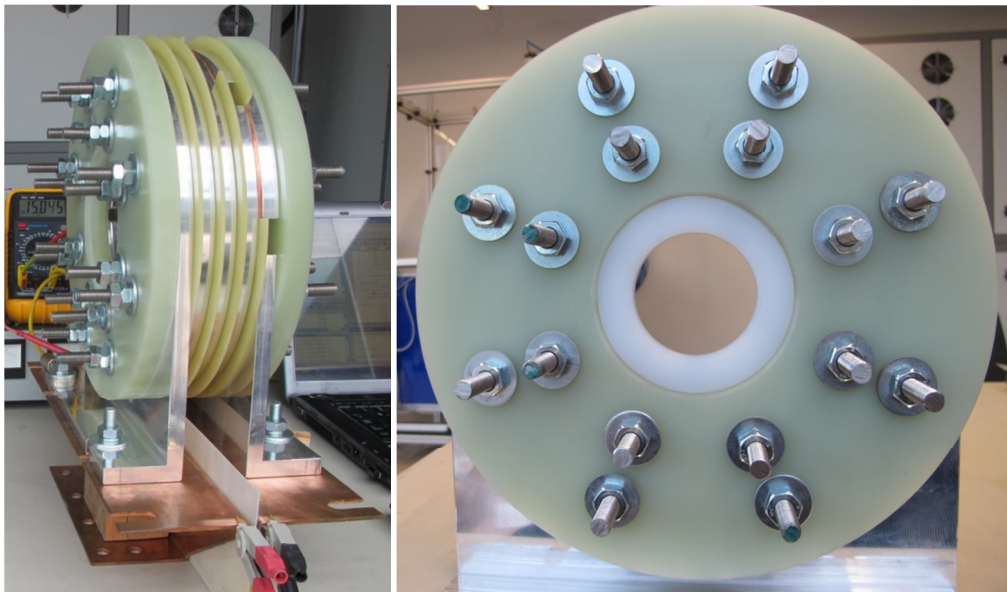


**Figure 10:** Newly designed prototype coil

### Manufacturing of a cylindrical helix coil prototype

EELAB designed a helix coil prototype. In this section, the preparation and building steps required for the Helix wire wound tool coil are discussed. It starts with the preparation of the coil former (the base) on which the conductors are wound. The following step is the winding of the conductors with a rectangular cross section. A layer of polyester resin with glass fibre filler is used for equalizing the level for the glass fibre reinforcement material.

Some pictures of the coil are shown in Figure 11.

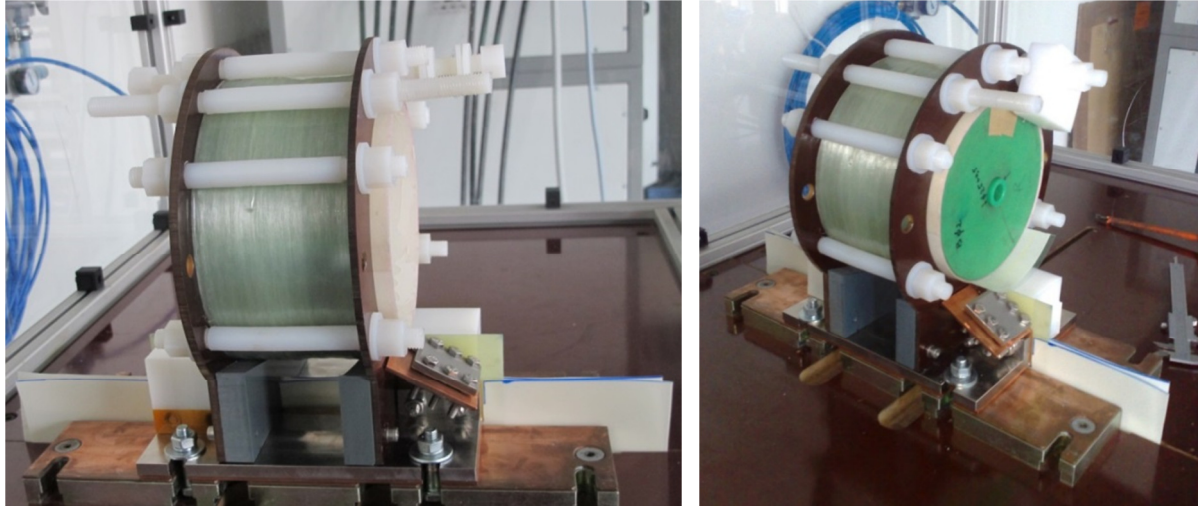


**Figure 11:** Helix prototype coil

### Demonstration workpieces for cutting and flat forming

Demonstration work pieces for flat forming were selected to set up a feasibility demonstration for embossing by electromagnetic forming. The embossing demonstrator workpiece has a size of 300x160 mm and the embossing area is about 180x90 mm. In Figure 12, results of individual tests are presented. However, the major intention of these experiments was testing the inductor performance. Extended experimental studies regarding the process design and optimisations were out of the scope of the project.

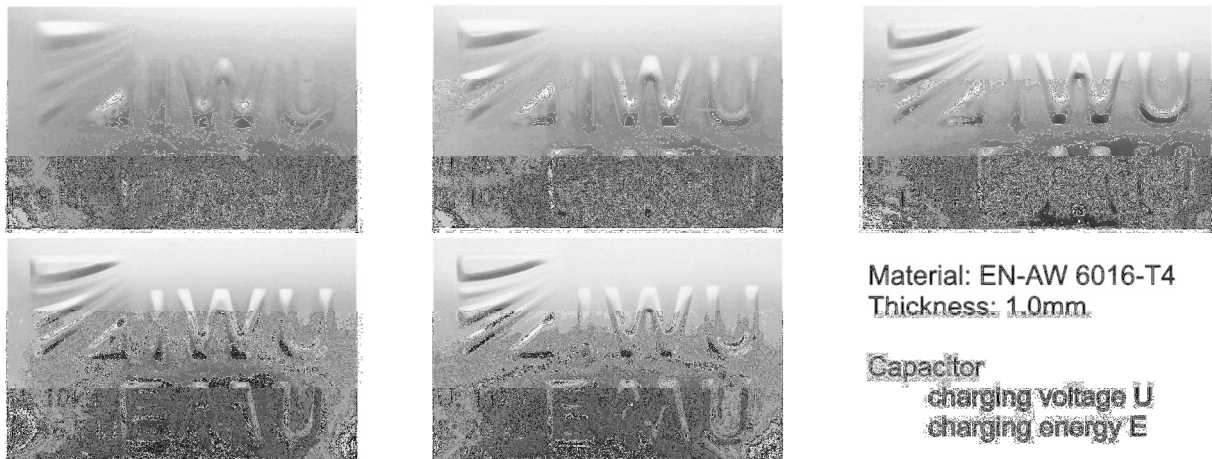


**Figure 12:** Series of embossing tests with different charging energies

It can be observed, that as expected, the incisiveness increases with increasing capacitor charging energy. Furthermore, it is obvious that a minimal size of the embossing element (e.g. of the letter and symbol size) is necessary. In the presented cases, embossing elements with a width of less than 5 mm could not be formed to a satisfying degree and increasing the charging energy showed no remarkable improvement.

Disagreeing with the expectations, random tests performed on workpieces with severely different wall thickness have shown that the minimum possible embossing element size is not significantly influenced by the sheet thickness. In experiments performed on sheets of 1 mm thickness and 0,6 mm thickness, respectively, are compared. It can be seen that the deformation is qualitatively similar. In case of the thinner sheet, lower charging voltage and energy respectively is required. This

effect might be attributed to the thickness and the according mass and stiffness of the sheet. However, a quantitative comparison of the applied energies is not reasonable here, because the sheets are made of different aluminium alloys and feature accordingly different material strengths. Nevertheless, it is interesting that despite of the different wall thicknesses, the same embossing elements are formed or not formed.



Material: EN AW-3103-T4  
Thickness: 0,6mm

Capacitor  
charging voltage 7kV  
charging energy 8kJ



Material: EN AW-6016-T4  
Thickness: 1,0mm

Capacitor  
charging voltage 9kV  
charging energy 13,5kJ

**Figure 13:** Embossing test with dependency of the sheet metal thickness. It should be noted that different materials and charging energies are used

Fraunhofer IWU used cutting demonstrators for basic investigations and technology oriented investigations (Figure 14).

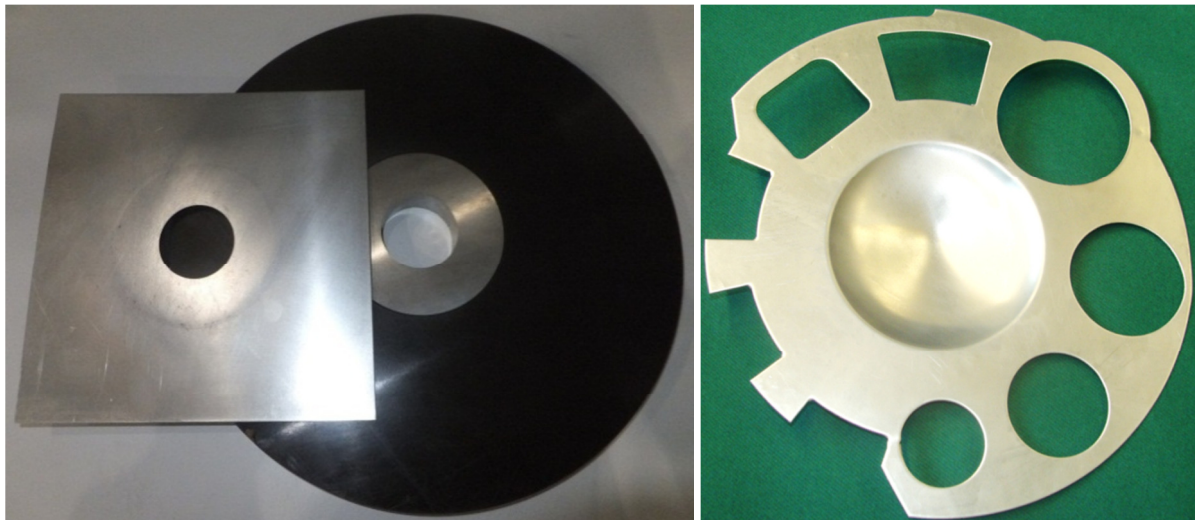


**Figure 14:** Cutting demonstrators. Left: Basic investigations. Right: Technology oriented investigations

Basic investigations comprised the cutting of diameters  $\varnothing 35$  up to 100 mm. Aluminium AA6016-T4 and steel DC04 in the thickness 1,0 and 0,6 mm respectively were tested. The objective was to investigate the impact of process parameters like charging energy and magnetic pressure and to characterise the process by appropriate quantities. For technology oriented experiments, a demonstrator showing different design elements was used. The outer diameter is about 350 mm. This demonstrator was used together with a helical flat coil which has an operation diameter of 400 mm.



**Figure 15:** Left: Influence of neighbouring cutting elements. Right: Remaining radii in sharp edges

The objective was to show the characteristic of cutting multiple cut-offs within one single pulse. The results clearly show that in principle, it is possible to cut multiple elements including the outer contour of the component. However, in case of small distances neighbouring cuttings can mutually influence each other. This is exemplarily shown in Figure 15 on the example of the circular cut-off and the outer line.

It has to be noticed that compared to the other circular cut-outs the roundness of this one is shows stronger deviations. A possible explanation for this effect is that the cut of both elements (circle and outer contour) did not happen in exactly the same moment. The outer line of the work piece was probably cut shortly after the circular hole. This means that the forces leading to the material detachment at the outer contour also deformed the narrow edge of the circular cut-out. With increasing distance between the individual elements this influence is reduced, because due to the high velocities, there is not enough time to draw material into the forming/cutting zone. So in principle the EMF process is more related to stretch drawing than to deep drawing.

The right picture in Figure 15 shows a remaining radius of about 1 mm despite actually sharp die corners. Depending on the material, it is furthermore possible that an unclear cutting is visible in such sharp corners. Comparing experiments with different charging energies, it can be seen that after exceeding the minimum required energy and pressure for cutting, a further increase of the energy initially leads to more precise cutting of small radii and sharp corners. However, after passing a threshold value even further increased energies show minor and finally negligible effects, only.

### **Demonstration workpieces for joining of tubular products**

The magnetic pulse welding process is a "cold" welding process; the heat generation is very limited. The process will create no or a very small heat-affected zone. The absence of heat during the operation allows joining materials with strongly different melting points. It is for example possible to weld aluminium to copper, aluminium to steel or copper to brass. A weld cross section shows many similarities with that of an explosion-welded joint (see Figure 17 and Figure 18).

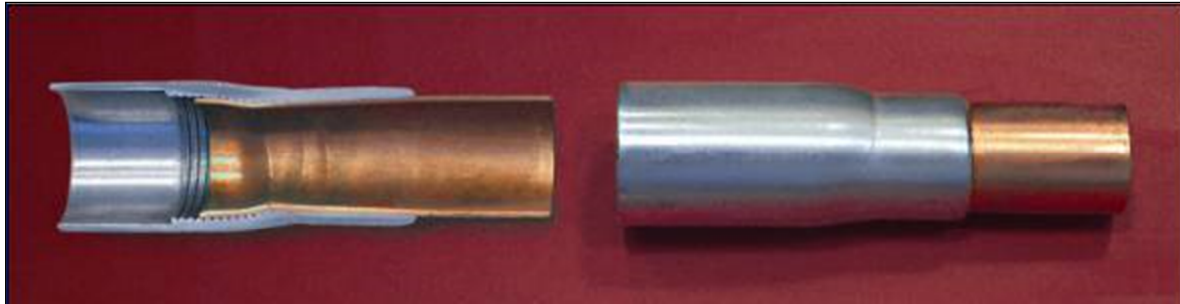


**Figure 16:** Electromagnetic pulse weld of an aluminium to a copper tube (Source: Pulsar)

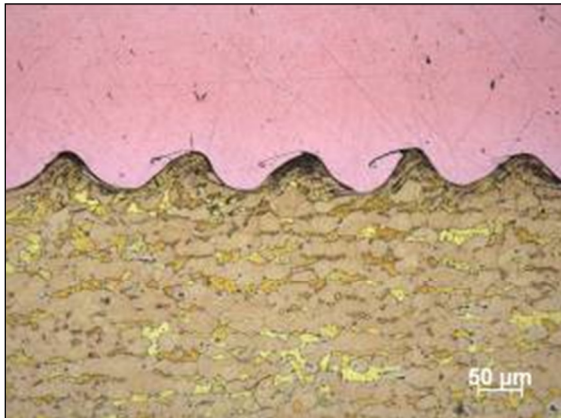


**Figure 17:** Cross section of a magnetic pulse weld of copper to brass (Source: BWI-CEWAC project SOUDIMMA)



**Figure 18:** Cross section of a magnetic pulse weld of copper to brass - Detail of Figure 17 (Source: BWI-CEWAC project SOUDIMMA)

Applications can be found for materials that are difficult to weld with the conventional welding techniques. For example, copper and aluminium are materials which usually can only be joined by brazing or soldering, but these processes are labour intensive and therefore expensive. Other sectors that examine the use of the electromagnetic pulse process for their applications are the aerospace and the nuclear sector, where very specific heat-resistant materials are used.

Other applications include the copper pipes in refrigeration systems, which can be joined using magnetic pulse welding (Figure 19).

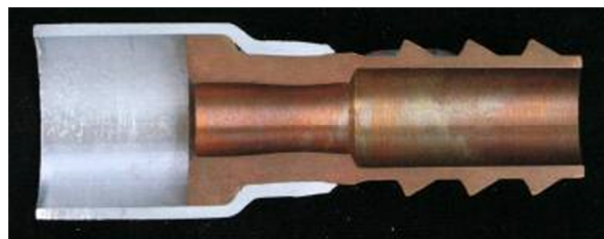


**Figure 19:** Connection of an aluminium to a copper tube (Source: SLV Munich)

To prove its suitability and applicability, the described inductor design strategy was used for configuring an inductor system for magnetic pulse welding. The manufacturing task was welding of dissimilar metals by compression. As mentioned above, the impacting conditions are the relevant criteria for magnetic pulse welding. The impacting angle depends on the geometrical design of the internal part, so that this optimisation is regarded in the experimental phase of the design process. During the first design steps the focus is put on adapting the impacting velocity. According to literature, velocities of 300-400 m/s should be beneficial with regard to welding aluminium to steel.

### **Deduction of a suitable pressure pulse**

A numerical parameter study was performed to identify a suitable pressure pulse for achieving the desired impacting velocity. The pressure distribution acting on the outer joining partner was assumed as a piecewise linear function, the temporary course was approximated by the first half-wave of a sinusoidal oscillation. Strictly speaking, a function corresponding to the square of a sinusoidal oscillation might be slightly more correct, but this causes only marginal differences. Amplitude  $p_{\max}$  and frequency  $f$  of the oscillation were varied in the parameter study.

As expected, higher pressure amplitudes cause higher impacting velocities. For the regarded setup, the desired range of impacting velocities of 300-400 m/s can be achieved by applying pressure amplitudes of at least 250 MPa. Moreover, there is a pressure-dependent frequency optimum, for which maximum impacting velocities can be achieved at the same pressure amplitude. Approximating this optimum improves the energy efficiency of the process tentatively allowing higher production rates and definitely reducing the loading of the inductor system.

From this study, the objective is a pressure pulse with a maximum of 250 up to 400 MPa and corresponding to a frequency preferably in the range of 10-25 kHz but not lower than 8 kHz. Considering the strength of typical inductor materials, aiming at higher pressures is not reasonable.

### **Preliminary design via decoupled simulation**

For directly acting inductors, the inner diameter is determined by the workpiece diameter and the gap width, required for secure insulation. The total length of the winding should be slightly longer than the length of the pressurized area, and the gap between the individual turns depends on the required insulation thickness. Thus, the only possibility for inductor optimization is changing the number of turns together with the width of the individual turns. Contrary, if a fieldshaper is applied, the diameter of the concentrating area is determined by the workpiece diameter and the insulation gap and the length of the concentrating area should be slightly longer than the joining area, but the inductor winding can be chosen freely as long as secure insulation of the individual turns is guaranteed.

The evaluation was performed regarding the target pressure pulse. The magnetic fields were calculated using the free two-dimensional FE-simulation tool FEMM 4.2. The inductor current was approximated by harmonic sinusoidal oscillation.

### **Demonstration workpieces for joining of tubular products**

Welding experiments were performed in order to evaluate the developed coil. Various material combinations were tried :

- copper - brass,
- aluminum - mild steel,
- aluminum - copper,

In the list above, the first mentioned material is the outer tubular material. The experiments were performed with solid internal workpieces. The tubes had an outer diameter of 25 mm and wall thicknesses of 1,5 mm. For example, a weld of an aluminum tube with a steel internal workpiece is shown in Figure 20.

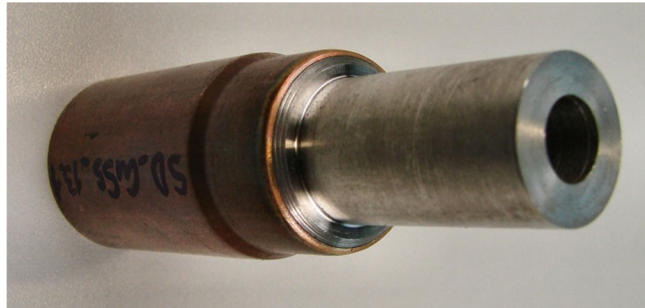


**Figure 20:** Copper-steel weld (tube diameter: 25 mm, wall thickness: 1,5 mm)

The weld quality was assessed by means of metallographic examinations. Hereto, the welded zone of each workpiece is isolated and cross-sectioned.

The process parameters for joining the tubes to the solid workpieces were optimised experimentally. The optimisation was performed based on the measurement of the length of the welded zone. The weld length was defined as the average value of the weld lengths measured at two sides of a metallographic specimen.

A weld joint can be divided in 3 zones. An example of a copper-brass joint is shown in Figure 21. Actual welding of the materials only occurs in the middle part of the weld zone. As the tube will impact the solid workpiece from left to right in this figure, the zone at the left without weld formation, is called the run-in zone. The right zone is called the run-out zone. The notches created in these areas can be very detrimental in case of dynamic loads or in corrosive environments.

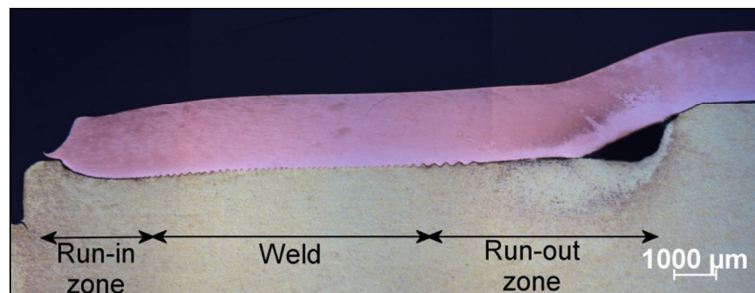


**Figure 21:** Metallographic section of a typical copper-brass weld

Generally, the internal workpieces are severely deformed by the impact. The most pronounced deformation occurs in the run-in zone. From there on, the deformation of the internal workpiece gradually declines towards the end of the weld (from left to right in Figure 21). This experimental observation proves that the impact of the tube first occurs at the run-in zone. The indentation in this zone is found to be between 0,5 and 1,0 mm. At a lower energy level or with a smaller air gap width, the deformation decreases. The width of this severely deformed zone increases for a longer overlap of the field shaper with the tube. These high deformations show that in case a tube is used as internal workpiece, an internal support should be applied to prevent deformation.

For some material combinations, a wavy weld interface is observed, more specific for the combinations aluminum-aluminum, copper-brass, copper-steel and copper-stainless steel. In Figure 22, a macrographic section of a copper-steel weld is shown. The other material combinations have a flat or nearly flat weld interface. As an example, the weld interface of a copper-aluminum weld is shown in Figure 24. The wave formation process is however not mandatory for a good bonding, as stated by some authors. Moreover, waves can also be observed in regions where no bonding occurred.

The wavy pattern is also observed in joints realized by explosion welding. This transition zone between the materials is believed to be caused by mechanical mixing, intensive plastic deformation and/or local melting. Temperature increase at the weld interface occurs due to Joule heating, the collision of the two workpieces and the jet formation.

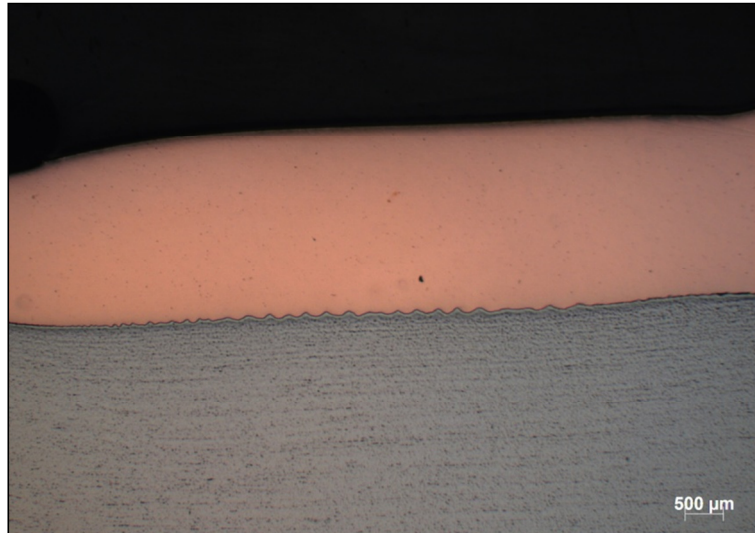


**Figure 22:** Metallographic section of a typical copper-steel weld



**Figure 23 :** Wavy weld interface of a copper-steel weld (detail of Figure 22)

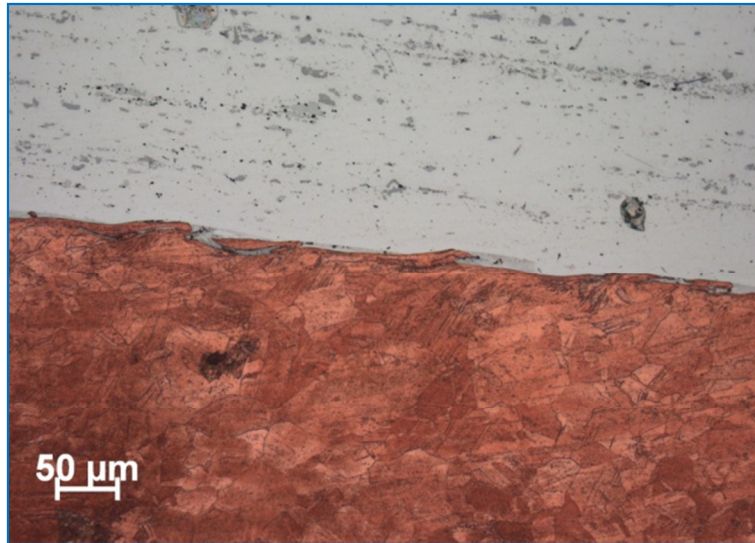


*Figure 24 : Weld interface of a copper-aluminum weld (with a small and flat intermetallic layer)*

### Summary and outlook

To make the technological advantages of EMF processes applicable in industrial manufacturing, a 3-step design strategy for inductor systems was developed. First simplified decoupled mechanical and electromagnetic simulations are applied for creating a preliminary design. For a clearly structured approach, a systematic iterative optimisation procedure was suggested. Then, coupled simulations proof the preliminary design and allow further improvements, if necessary. Thus, the overall numerical costs can be reduced. For challenging design tasks, a prototypic implementation of the inductor system serves as verification and for final experimental optimisation. First proof of the basic feasibility of the design strategy is given by applying it for designing an inductor system for magnetic pulse welding of tubes. Further verification of the design principle shall be given in a future more detailed analysis of the welding process including velocity measurements.